PAPER

www.rsc.org/loc

"Microcanals" for micropipette access to single cells in microfluidic environments

Chia-Hsien Hsu,[b] Chihchen Chen[a] and Albert Folch*[a]

[a] *Department of Bioengineering, University of Washington, Seattle, WA 98105, USA. E-mail: afolch@u.washington.edu; Fax: +1 206543 6124; Tel: +1 206 685 22577*

[b] *Department of Mechanical Engineering, University of Washington, Seattle, WA 98105, USA*

Received 1st April 2004, Accepted 26th April 2004
First published as an Advance Article on the web 23rd July 2004

We demonstrate the fabrication and operation of "microcanals" (*i.e.* open-air microfluidic channels without a roof), which enable micropipette manipulation and probing of cells within a microfluidic environment. The microcanal devices are fabricated in PDMS on glass substrates using a PDMS membrane transferring technique. Here we show patch-clamp electrophysiological recording and intracellular dye injection performed on cells seeded in microcanals.

Introduction

Microfluidic devices offer several salient features that are advantageous for biomedical applications: (1) the consumption of costly reagents and the handling of hazardous materials is minimized; (2) parallel operation; (3) reaction times are shortened due to the large surface-to-volume ratio in microfluidic environments; (4) microfluidic scales are comparable to those of single cells, thus single-cell-level experiments are possible; and (5) liquids flow laminarly in microfluidic channels without turbulence,[1] allowing for sub-cellular studies[2,3] and straightforward modeling of flow conditions in cell-containing microchannels.[4] A large number of microfluidic systems have been reported for genomic and proteomic analysis,[5] micropatterning of proteins,[6–8] and cells,[7–10] protein crystal growth,[11] single-cell manipulation,[12–16] microvascular research,[17] cell-based biosensors,[18,19] and microanalytical systems,[20–28] to name a few applications. Present microfluidic devices, however, suffer from an inherent limitation for a certain class of cell-based studies: the inaccessibility of cells cultured in closed channels precludes the use of micropipettes. While micropipette operation is labor intensive and yields low throughputs, micropipettes are, on the other hand, readily available in vast numbers of biomedical laboratories and effectively constitute an inexpensive nanotechnology tool (apertures of submicron diameter are straightforward to produce with a commercial pipette puller) of unique versatility. As such, they have been widely used for decades for single cell injection (reviewed in ref. 29), patch-clamp electrophysiology (reviewed in ref. 30), iontophoretic stimulation[31,32] (reviewed in ref. 33), and "puffing" (pressure ejection to form gradients) of signaling factors (reviewed in ref. 33). In addition, micropipettes can be used for mechanical manipulation of single cells, *e.g.* to bring a given cell into contact with other cells for secretion studies[34] or to sever a portion of the cell membrane for cellular transport studies,[35] among other applications. Micropipettes are routinely combined with custom-made or commercially-available macrofluidic perfusion setups which do not feature the advantages of microfluidic perfusion mentioned above. Here we demonstrate the integration of microfluidic and micropipette technologies in one same platform consisting of microfluidic streams that are open to air (*i.e.* microchannels without a roof or "microcanals") and that, as a result, are compatible with micropipette manipulation and probing of single cells. Open-air microfluidic systems have been reported before. Columbus and Palmer discussed the utility of "fluid bridges" for potentiometric analytical devices;[36] others have used open-air reservoirs that take advantage of evaporation for pumping fluids,[37] concentrating reagents,[38] or improving the microenvironment of cells in (capped) microfluidic channels.[39] An obvious drawback of our integrated platform is that it is not amenable to high-throughput studies. Several groups have shown specialized solutions to the throughput limitations of pipettes, such as patch-clamp chips[40–45] or automated fluid gradient generators,[43] but the functionality of these specialized devices is not as broad as that of micropipettes. Here we demonstrate two micropipette functionalities (intracellular injection and patch-clamp recordings) in one same microfluidic platform.

Fabrication method

Our microfluidic device is made by molding in polydimethylsiloxane (PDMS) using soft lithography techniques.[46] PDMS is an attractive material for making microfluidic systems[47] for several reasons: (a) the elasticity of PDMS allows for easy, nondestructive release and replication from (reusable) molds; (b) PDMS is transparent down to a wavelength of 300 nm, so it can be combined with most optical detection methods (*e.g.* fluorescence and phase-contrast microscopy); (c) PDMS is inexpensive, inert and biocompatible;[48,49] (d) it bonds to smooth surfaces by reversible conformal contact and can also be irreversibly bonded to any hydroxy-terminated surface (such as glass) after a brief oxygen plasma treatment.[50] In our device, the cells are cultured on glass and the PDMS device is irreversibly bonded to the glass surface; thus, the microcanals consist of a glass floor and PDMS walls (ranging 50–200 μm wide and 50–200 μm tall, depending on the device). Glass is our choice of microcanal floor material because it is commonly used in cell culture studies and is amenable to surface chemical derivatization for cell patterning studies.[51] The PDMS walls of the microcanals and the rest of the device (which contains traditional microchannels with roof) form a three-dimensional (3-D) architecture of stacked PDMS layers. A number of researchers have reported 3-D microfluidic systems that are fabricated by stacking and aligning several thin, patterned PDMS layers.[8,50,52] Thin PDMS layers are not easily handled and/or aligned without deforming their features; hence the

DOI: 10.1039/b404956j

particulars of the handling method are important for constructing multilayer PDMS microfluidic devices. The fabrication of the device is illustrated in Fig. 1a–f. A master wafer was made using conventional photolithography with a negative photoresist (SU-8, Microchem Inc., Newton, MA). PDMS prepolymer (SYLGARD 184 Silicone Elastomer Kit, Dow Corning, Midland, MI) mixed with curing agent was dispensed on top of the master (Fig. 1a). A fluoropolymer coated polyester (PE) sheet (Scotchpak™ 1002 Release Liner, 3M™, St. Paul, MN) and glass plates were applied and pressed against the master so as to exclude PDMS prepolymer from the top of the SU-8 features (Fig. 1b and c); the glass plates simply serve the purpose of transmitting even pressure to the PE sheet. Once the excess PDMS was squeezed out, the PDMS trapped between the master and the PE sheet was cured at 65 °C in an oven for 2 h. Once cured, the PE sheet adhered to the PDMS features, which could be removed from the master along with the PE sheet without apparent distortion (Fig. 1d); we have not attempted to quantify the distortion because it is not obviously appreciable under microscopic observation in comparison with our smallest (50 μm wide) microcanals. The PDMS layer and a glass substrate were both treated with oxygen plasma and brought into physical contact. The PDMS layer irreversibly bonded to the glass, whereas the PE sheet was peeled off the PDMS without damaging it (Fig. 1e and f). Finished PDMS devices with 200 μm wide microcanals assembled on a glass substrate are shown in Fig. 1g–h. We note that the choice of fluoropolymer-coated PE as the material for the backing sheet is important. To begin with, fluoropolymer-coated PE binds to cured PDMS strongly enough to remove it from the master structures but weak enough for the PDMS layer to be transferred to (oxygen plasma-activated) glass without apparent damage to either the PDMS or the PE sheet's surfaces. We have not investigated whether this convenient, intermediate-strength PE-to-PDMS bond is of a physical or chemical nature. In addition, the PE sheets are also important from a mechanical point of view: with the support provided by PE sheets, thin PDMS membranes can be manually handled with a minimum amount of sagging and distortion. However, alignment errors can still be introduced during the layer-to-layer stacking process. To reduce the number of the molding and aligning steps, we fabricated masters that already contain features of different heights made by multiple-layer photolithography. Thus, certain 3-D PDMS structures, such as networks incorporating both microchannels and microcanals, can be made in a single molding process, as illustrated in the Fig. 1a–f schematics.

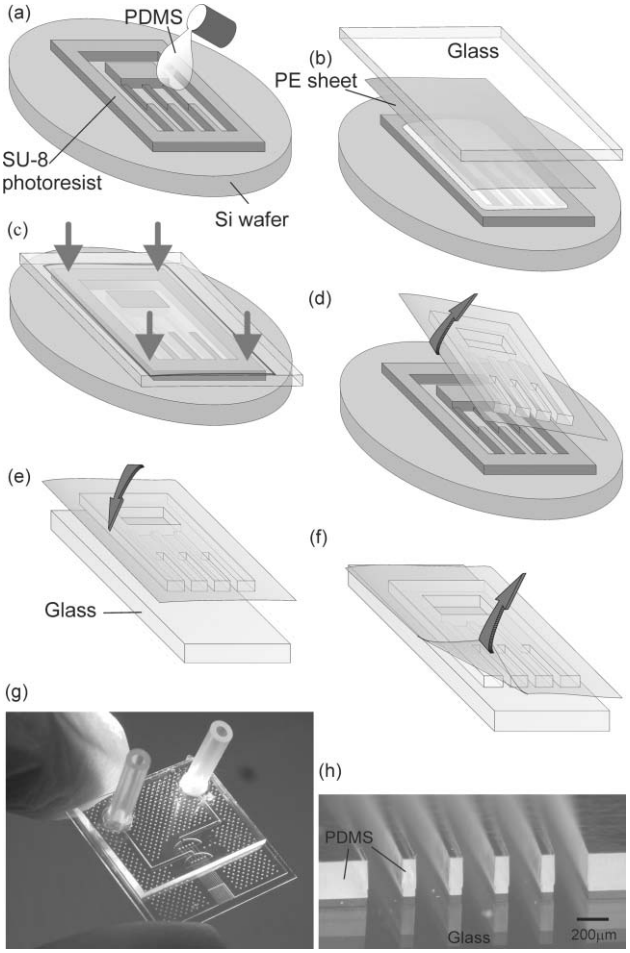

Fig. 1 (a) A master silicon wafer was created using SU-8 photoresist and standard photolithography procedures. (b) and (c) PDMS prepolymer mixed with curing agent was dispensed on top of the master. A PE sheet and glass plates were applied and pressed against the master. (d) The PDMS was cured and peeled off from the mold along with the PE sheet. (e) The PDMS membrane and a glass substrate were both treated with oxygen plasma and chemically bonded together. (f) The PDMS membrane irreversibly bonded to the glass surface, which allowed for the PE sheet to be peeled off from the PDMS. (g) An image of a microcanal device with two inlets and fluidic circuit on a cover slide. (h) An image of the exit area of a microcanal device.

Results and discussion

Fluid operation

Fig. 2 shows microcanal devices in operation. The microcanal device can be used for different applications depending on the actual design of the upstream network. Fig. 2a shows a set of microcanals that were all filled with red dye, requiring simple 2-D fluid distribution from the macroscopic inlet into the microchannels. On the other hand, Fig. 2b and c show more complex flow patterns that require 3-D fluid distribution networks upstream of the microcanal area. Fig. 2b shows heterogeneous laminar-flow streams in microcanals. Heterogeneous streams are widely used for sub-cellular analysis; they have been implemented in commercially-available macrofluidic setups (*e.g.*, the Dynaflow™ system) as well as in microfluidic setups,[3] in which multiple streams flow side-by-side in laminar flow. In Fig. 2b, each microchannel is fed through three

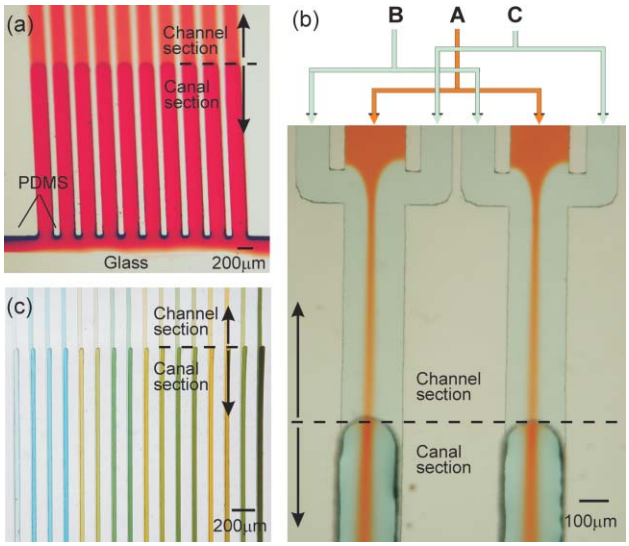

Fig. 2 (a) Photograph of a set of ten microcanals filled with a red dye solution. (b) Heterogeneous flow in microcanals; the two side streams (cyan, labeled B and C) hydrodynamically focus the center stream (orange, labeled A). (c) Combinatorial flows in microcanals; the picture shows sixteen microcanals, each inheriting unique concentrations of fluids from a combinatorial micromixer upstream (not shown).

different inlets using a 3-D network (schematized on top of Fig. 2b), such that the left, center and right inlets feed the left, center and right laminar streams, respectively, in all the microchannels and microcanals. This results in microfluidic focusing of the center stream, and the width and position of the center stream can be modulated dynamically by changing the flow rates of the left and right streams. As shown in Fig. 2c, the microcanals can also be filled with combinatorial mixtures for high-throughput testing experiments. Each microcanal of a set of sixteen inherits a unique mixture of two dyes (blue and yellow) at four different concentrations each; all the combinations of green (including pure blue, pure yellow and water) are achieved with an upstream combinatorial micromixer that has only two dye inlets.[53] Remarkably, when the flow exits the microchannels into the microcanals, the flow is confined within the two PDMS walls and the glass floor in the absence of a roof. A similar system that demonstrates flow confined between a microchannel's roof and floor and two fluid-air interface walls has been reported by Zhao *et al.*[54] As in Zhao *et al.*'s work, in our microcanals a differential surface wettability is crucial for fluid confinement (*i.e.* to avoid spilling onto adjacent microcanals). In our case, the vertical faces of the PDMS walls and the glass floor are hydrophilic (they were exposed to an oxygen plasma[47,50]), but the horizontal top surface of the walls separating microcanals is hydrophobic (it was bonded to the PE sheet throughout the plasma oxidation step). The hydrophilicity of the floor and the vertical part of the walls aids in filling the (dry) microcanals for the first time, and the hydrophobicity of the top surface of the PDMS walls prevents the fluid from spilling, pinning it at the edges. Thus, the fluid–air interface pinned by the PDMS hydrophobic surface constitutes a "virtual roof" for the flow. Shown in Fig. 3(a) is the measured flow rate per microcanal as a function of driving pressure using a five-microcanal device. The flow rate is proportional to the driving pressure, as predicted for a classical "pipe" (or microchannel),[1] indicating that the fluid–air interface acts as a solid roof for these flow rates and microchannel geometry.

To characterize the spilling point, we constructed devices with only one microcanal (of one of nine combinations of three different widths and three different depths in each device) and injected known flow rates through the inlet; the average flow rate was increased gradually, and the flow velocity value for which overflowing occurred (as judged by a human observer under a microscope) was recorded ("spilling velocity"). (Flow velocity is calculated by dividing the flow rate by the rectangular cross-sectional areas.) We found that the spilling velocity depends on (1) most dramatically, the method used to drain the fluid at the outlet of microcanals; (2) the width of the microcanal (we compared $w = 100$, 200, and 300 μm); and (3) least importantly, the height of the microcanal (we compared $h = 50$, 80, and 100 μm). We quantitatively compared two draining methods: (A) direct aspiration of excess fluid with a pipette tip connected to house vacuum ("aspiration drain"); and (B) capillary wicking of excess fluid by means of a 1 mm thick piece of tissue paper placed manually placed against the outlet ("wicking drain"). If the aspiration drain is used, the spilling speeds are often higher than what our pumps could provide; for some applications, however, aspiration with vacuum may not be adequate or possible. As an example, a 200 μm wide microcanal with 80 μm tall PDMS sidewalls can accept average flow speeds of up to 25 cm s^{-1} if aspiration drain is used, but only up to 4 cm s^{-1} if wicking drain is used. Similarly, 300 μm wide microcanals accepted so much flow, even with the wicking drain, that they could not be forced to spill reliably with our pumping equipment. Measurements of spilling flow rate and spilling speed on 100 μm and 200 μm wide microcanals using the wicking drain are plotted in Fig. 3b and c, respectively, as a function of microcanal height. A trend is

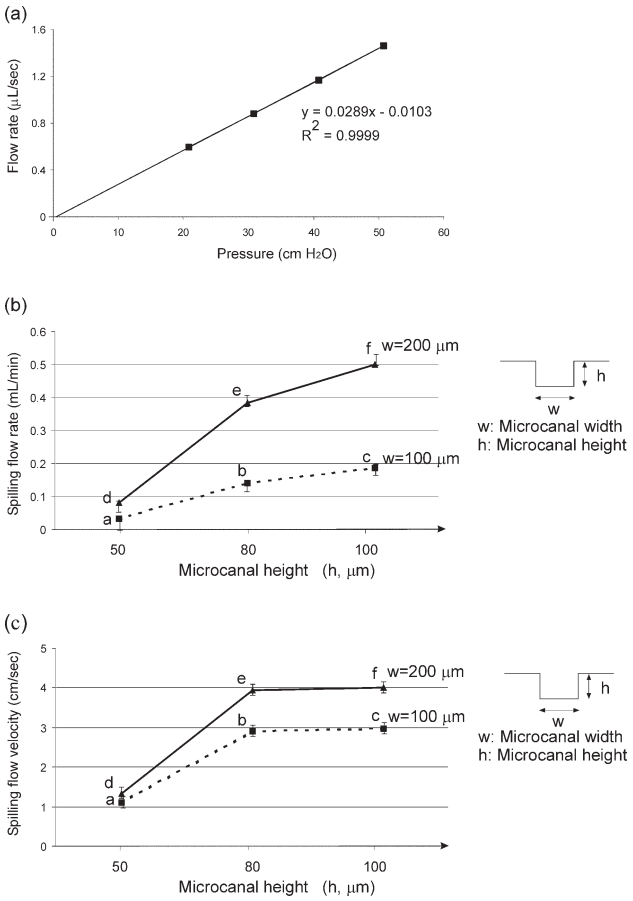

Fig. 3 (a) A plot of flow rate *vs.* driving pressure measured using gravitational perfusion of a 200 μm wide microcanal with 120 μm tall PDMS sidewalls. (b) A plot of measured spilling flow rate *vs.* microcanal sidewall height (h) for microcanal widths $w = 100$ or 200 μm. (c) A plot of spilling flow velocity *vs.* microcanal sidewall height (h) for microcanal widths $w = 100$ or 200 μm. For $w = 300$ μm, our pumps were not able to generate enough head pressure to cause the microcanals to burst at the open air interface.

observed that spilling flow rate increases with both microcanal width and height. A similar trend is observed for the spilling flow velocity. Interestingly, the spilling flow velocity (unlike the spilling flow rate) does not change appreciably with canal depth for the deeper (80 and 100 μm deep) microcanals.

Taken together, our observations indicate that the drain (even the wicking drain) can be an important component of the total flow resistance encountered by the fluid. We observed that the water stream coming out of a microcanal forms a thin flow layer on top of the tissue paper. This means that, when 1 mm thick tissue paper is used as the wicking drain, the fluid exiting a 50 μm deep microcanal has to "climb" more than the fluid exiting 80 μm or 100 μm deep microcanals. As a result, the virtual roof of a 50 μm deep microcanal is at a higher inner pressure than the roof of a 80 μm or a 100 μm deep microcanal, thus the flow appears to spill at a lower driving pressure (and hence a lower spilling velocity).

It is important to note that the values of spilling flow velocity reported here are far above the range in which cell studies would apply. Typically, laminar shear stress of the order of 0.5 to 10.0 N m^{-2} may remove adherent cells from surfaces.[55] We do not have a method to predict/measure the actual shear stress on the microcanal walls. However, when water flows at the speed of our spilling velocities in microchannels of cross-sectional dimensions equivalent to those of the microcanals used in our measurements, the wall shear stress is ~14,000 to 33,000 N m^{-2};[56] which is more than three orders of magnitude larger than the shear stress applicable to cells.

Micropipette probing and modification of single cells

Microcanals constitute a microfluidically-addressable cell culture environment that is accessible with micropipettes. Cells can be seeded in the microcanal floors simply by adding a cell suspension to the corresponding inlet and arresting the flow during cell attachment/spreading. Care must be taken to ensure that the microcanal is in a high-humidity sterile environment (such as an incubator) during the seeding procedure to prevent contamination and evaporation, which can be devastating to the cells because it readily alters the balanced composition of the cell culture medium. Once the flow is re-started, constant perfusion (*e.g.* provided by gravity flow from a sterile bottle) ensures that the cell culture medium in the microcanals is replenished continuously and is kept sterile (the time of residence of fluid in the whole device is orders of magnitude smaller than a typical bacterium's reproductive cycle). Patch-clamp electrophysiological recordings[30] from human embryonic kidney (HEK) cells performed in microcanals are shown in Fig. 4. HEK cells are widely used as an expression system in studies of ion channels. To characterize endogenous outward currents (I_m) in a native HEK cell, the membrane potential of the cell was held at −80 mV and changed with a series of step pulses from −100 to 70 mV with 10 mV increments (Fig. 4b top graphs). Currents and current-to-voltage relationships recorded from a HEK cell with a single micropipette and in the same microcanal at two different extracellular K^+ concentrations (5.4 mM and 20 mM KCl) are shown in Fig. 4b. The perfusion with 5.4 mM KCl lasted 30 s, after which 20 mM KCl was introduced in the same inlet of the device by switching a valve upstream (~10 cm fluid path to the inlet) of the tubing connected to the device. A shift of the reversal potentials (ΔV_r, see Fig. 4b) of ~20 mV is observed, indicating that the endogenous outward currents were partially carried by K^+, which is in agreement with previously reported results in traditional perfusion steps.[57] This experiment also demonstrates that fluids in microcanals can be switched promptly and smoothly to study different cellular responses without breaking the tight, delicate "gigaohm" seal[30] between the micropipette and the cell.

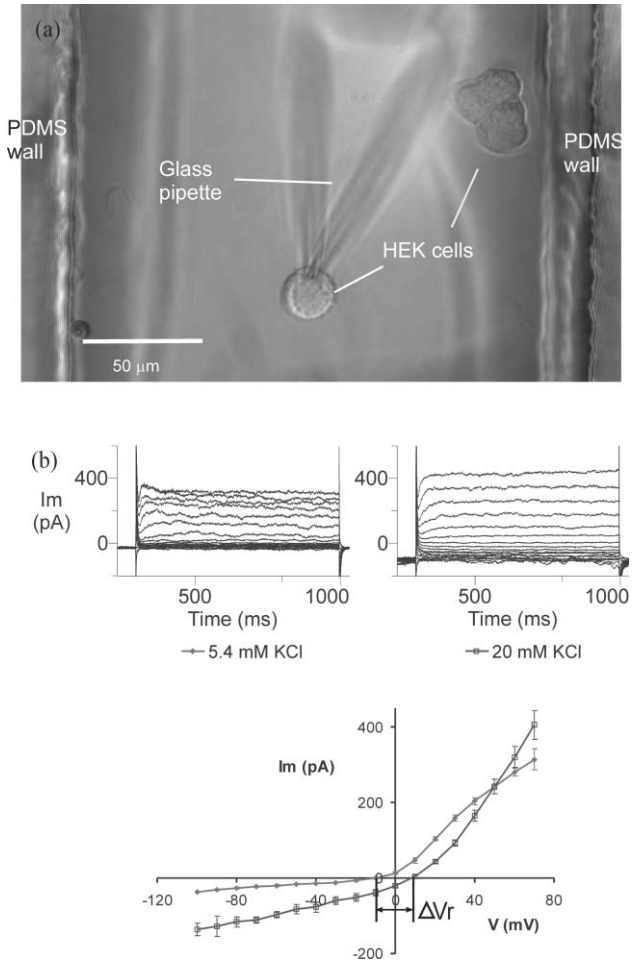

Fig. 4 (a) Micrograph showing a micropipette during whole-cell recordings of a HEK cell in a microcanal. (b) Representative current traces and I-V relationships recorded from a HEK cell at two different extracellular K^+ concentrations (5.4 mM or 20 mM) flowing in the microcanal.

As another demonstration that cells can be manipulated with micropipettes in the microcanals, we performed intracellular dye injections on microcanal-confined NIH 3T3 fibroblasts as shown in Fig. 5a (magnified in Fig. 5b). The seeding procedure was essentially identical to that described above for the patch clamp experiments. Under continuous flow, we inserted micropipettes (with inner diameter ranging from 0.2 to 1.0 μm) loaded with (green-fluorescent) Alexa Fluor 488-dextran or (red-fluorescent) fluoro-ruby-dextran (Molecular Probes, Eugene, OR) into individual cells. The dyes were injected into cells by applying brief (~20 ms) air pressure pulses (~20 psi) using a pneumatic pump (WPI PV830, World Precision Instruments, Sarasota, FL).

Conclusion

In summary, we have developed a method for fabricating microcanals, *i.e.* open-air microfluidic channels. The flow can easily be kept confined to the microcanals due to the high surface tension of the fluid-air interface, which is pinned at the corners of the hydrophobic top surface of the microcanal walls. The microcanals constitute an open-air microfluidic environment that is accessible with micropipettes for single-cell probing and manipulation. Patch clamping recordings and intracellular injection of dyes are demonstrated in this article.

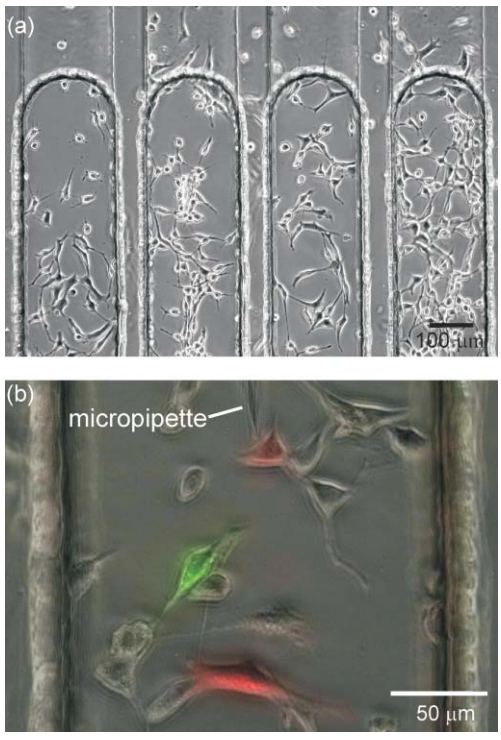

Fig. 5 (a) NIH 3T3 fibroblasts cultured in microcanals. (b) 20× overlays of the phase-contrast and fluorescence images of cell-containing microcanals, showing a few selected cells microinjected with Alexa Fluor 488-dextran (green) or fluoro-ruby-dextran (red).

Although the micropipette/microcanal technique necessarily reduces the high-throughput testing benefits that are typical of microsystems, it still takes advantage of other salient features of microfluidic devices such as small size, minimal reagent consumption, laminar-flow regime, and automated mixing/titration of complex solutions.

Acknowledgements

This work was supported by NSF (CAREER Award). The authors would like to thank the Washington Technology Center (WTC) for use of its clean room facilities and Dr Chris Neils for the combinatorial mixer used for Fig. 2c.

References

1 G. E. Karniadakis and A. Beskok, *Micro Flows*, Springer-Verlag, New York, 2002.
2 S. Takayama, J. C. McDonald, E. Ostuni, M. N. Liang, P. J. A. Kenis, R. F. Ismagilov and G. M. Whitesides, *Proc. Natl. Acad. Sci. USA*, 1999, **96**, 5545.
3 S. Takayama, E. Ostuni, P. LeDuc, K. Naruse, D. E. Ingber and G. M. Whitesides, *Nature*, 2001, **411**, 1016.
4 G. A. Ledezma, A. Folch, S. N. Bhatia, M. L. Yarmush and M. Toner, *J. Biomech. Eng.*, 1999, **121**, 58.
5 G. H. W. Sanders and A. Manz, *Trends Anal. Chem.*, 2000, **19**, 364–378.
6 E. Delamarche, A. Bernard, H. Schmid, B. Michel and H. Biebuyck, *Science*, 1997, **276**, 779–781.
7 A. Folch and M. Toner, *Biotechnol. Prog.*, 1998, **14**, 388–392.
8 D. T. Chiu, N. L. Jeon, S. Huang, R. S. Kane, C. J. Wargo, I. S. Choi, D. E. Ingber and G. M. Whitesides, *Proc. Natl. Acad. Sci. USA*, 2000, **97**, 2408–2413.
9 A. Folch, A. Ayon, O. Hurtado, M. A. Schmidt and M. Toner, *J. Biomech. Eng.*, 1999, **121**, 28.
10 A. Folch and M. Toner, *Annu. Rev. Biomed. Eng.*, 2000, **2**, 227–256.
11 A. Sanjoh and T. Tsukihara, *J. Cryst. Growth*, 1999, **196**, 691–702.
12 P. C. Li and D. J. Harrison, *Anal. Chem.*, 1997, **69**, 1564–8.
13 P. R. C. Gascoyne, X. B. Wang, Y. Huang and F. F. Becker, *IEEE Trans. Ind. Appl.*, 1997, **33**, 670–678.
14 S. Gawad, L. Schild and P. Renaud, *Lab Chip*, 2001, **1**, 76–82.
15 J. Olofsson, K. Nolkrantz, F. Ryttsen, B. A. Lambie, S. G. Weber and O. Orwar, *Curr. Opin. Biotechnol.*, 2003, **14**, 29–34.
16 J. Voldman, R. A. Braff, M. Toner, M. L. Gray and M. A. Schmidt, *Biophys. J.*, 2001, **80**, 531–541.
17 N. Sutton, M. C. Tracey, I. D. Johnston, R. S. Greenaway and M. W. Rampling, *Microvasc. Res.*, 1997, **53**, 272–281.
18 L. Bousse, *Sens. Actuators, B*, 1996, **B34**, 270–275.
19 X. X. Cai, N. Klauke, A. Glidle, P. Cobbold, G. L. Smith and J. M. Cooper, *Anal. Chem.*, 2002, **74**, 908–914.
20 S. C. Jacobson, L. B. Koutny, R. Hergenroder, A. W. Moore and J. M. Ramsey, *Anal. Chem.*, 1994, **66**, 3472.
21 L. B. Koutny, D. Schmalzing, T. A. Taylor and M. Fuchs, *Anal. Chem.*, 1996, **68**, 18–22.
22 L. C. Waters, S. C. Jacobson, N. Kroutchinina, J. Khandurina, R. S. Foote and J. M. Ramsey, *Anal. Chem.*, 1998, **70**, 158.
23 M. Koudelka, F. Rohner-Jeanrenaud, J. Terrettaz, E. Bobbioni-Harsch, N. F. de Rooij and B. Jeanrenaud, *Biomed. Biochim. Acta*, 1989, **48**, 953–6.
24 J. Cheng, E. L. Sheldon, L. Wu, A. Uribe, L. O. Gerrue, J. Carrino, M. J. Heller and J. P. O'Connell, *Nat. Biotechnol.*, 1998, **16**, 541–6.
25 G. Ocvirk, H. Salimi-Moosavi, R. J. Szarka, E. Arriaga, P. E. Andersson, R. Smith, N. J. Dovichi and D. J. Harrison, *Micro Total Analysis Systems '98*, 1998, 203–206.
26 J. Yakovleva, R. Davidsson, A. Lobanova, M. Bengtsson, S. Eremin, T. Laurell and J. Emneus, *Anal. Chem.*, 2002, **74**, 2994–3004.
27 R. Kurita, K. Hayashi, T. Horiuchi, O. Niwa, K. Maeyama and K. Tanizawa, *Lab Chip*, 2002, **2**, 34–38.
28 O. Hofmann, G. Voirin, P. Niedermann and A. Manz, *Anal. Chem.*, 2002, **74**, 5243–5250.
29 K. T. Brown, *Advanced Micropipettte Techniques for Cell Physiology*, Wiley, Chichester, 1986.
30 *Patch-Clamp Applications and Protocols*, ed. A. A. Boulton, G. A. Baker and W. Walz, Humana Press, 1995.
31 W. L. Nastuk, *J. Cell. Comp. Physiol.*, 1953, **42**, 249–272.
32 J. del Castillo and B. Katz, *J. Physiol.*, 1955, **128**, 157–181.
33 T. W. Stone, *Microiontophoresis and Pressure Ejection*, John Wiley & Sons, New York, 1985.
34 I. Chow and M. M. Poo, *J. Neurosci.*, 1985, **5**, 1076–1082.
35 D. Y. Gao, J. J. McGrath, J. Tao, C. T. Benson, E. S. Critser and J. K. Critser, *J. Reprod. Fertil.*, 1994, **102**, 385–392.
36 R. L. Columbus and H. J. Palmer, *Clinical Chemistry*, 1987, **33**, 1531–1537.
37 C. S. Effenhauser, H. Harttig and P. Kramer, *Biomed. Microdevices*, 2002, **4**, 27–32.
38 G. M. Walker and D. J. Beebe, *Lab Chip*, 2002, **2**, 57–61.
39 G. M. Walker, M. S. Ozers and D. J. Beebe, *Biomed. Microdevices*, 2002, **4**, 161–166.
40 N. Fertig, R. H. Blick and J. C. Behrends, *Biophys. J.*, 2002, **82**, 3056–3062.
41 H. Vogel, *Abstracts of Papers of the American Chemical Society*, 2001, **222**, U368–U368.
42 R. Pantoja, D. Sigg, R. Blunck, F. Bezanilla and J. R. Heath, *Biophys. J.*, 2001, **81**, 2389–2394.
43 N. L. Jeon, H. Baskaran, S. K. W. Dertinger, G. M. Whitesides, L. Van de Water and M. Toner, *Nat. Biotechnol.*, 2002, **20**, 826–830.
44 N. Fertig, M. Klau, M. George, R. H. Blick and J. C. Behrends, *Appl. Phys. Lett.*, 2002, **81**, 4865–4867.
45 T. Lehnert, M. A. M. Gijs, R. Netzer and U. Bischoff, *Appl. Phys. Lett.*, 2002, **81**, 5063–5065.
46 Y. N. Xia and G. M. Whitesides, *Angew. Chem.-Int. Edit. Engl.*, 1998, **37**, 551.
47 J. C. McDonald and G. M. Whitesides, *Acc. Chem. Res.*, 2002, **35**, 491–499.
48 M. C. Belanger and Y. Marois, *J. Biomed. Mater. Res.*, 2001, **58**, 467–477.
49 D. Fallahi, H. Mirzadeh and M. T. Khorasani, *J. Appl. Polym. Sci.*, 2003, **88**, 2522–2529.
50 B. H. Jo, L. M. Van Lerberghe, K. M. Motsegood and D. J. Beebe, *J. Microelectromech. Syst.*, 2000, **9**, 76–81.
51 A. Tourovskaia, T. Barber, B. T. Wickes, D. Hirdes, B. Grin, D. G. Castner, K. E. Healy and A. Folch, *Langmuir*, 2003, **19**, 4754–4764.
52 J. R. Anderson, D. T. Chiu, R. J. Jackman, O. Cherniavskaya, J. C. McDonald, H. K. Wu, S. H. Whitesides and G. M. Whitesides, *Anal. Chem.*, 2000, **72**, 3158–3164.
53 C. M. Neils, Z. Tyree, B. Finlayson and A. Folch, *Lab Chip*, 2004, **4**.
54 B. Zhao, J. S. Moore and D. J. Beebe, *Science*, 2001, **291**, 1023–1026.
55 J. Aunins and H. J. Henzler, *Aeration in Cell Culture Bioreactors*, VCH, Weinheim, 1993.
56 J. T. Keane, D. Ryan and P. P. Gray, *Biotechnol. Bioeng.*, 2003, **81**, 211–220.
57 B. Jiang, X. Sun, K. Cao and R. Wang, *Mol. Cell. Biochem.*, 2002, **238**, 69–79.